

Similarity renormalization group for nuclear forces

Matthias Heinz ^{a,b}

^aOak Ridge National Laboratory, National Center for Computational Sciences, Oak Ridge, TN 37831, USA

^bOak Ridge National Laboratory, Physics Division, Oak Ridge, TN 37831, USA

© 20xx Elsevier Ltd. All rights reserved.

Abstract:

Renormalization group methods generate low-resolution Hamiltonians that are more diagonal and easier to solve. This chapter reviews the similarity renormalization group for nuclear Hamiltonians, which is a popular method for generating low-resolution nuclear forces. It presents the similarity renormalization group flow equations, analyzes how the similarity renormalization group drives the Hamiltonian towards the diagonal, and studies the effect of induced many-body interactions. It concludes by highlighting the progress in first-principles calculations of nuclei driven by low-resolution nuclear Hamiltonians.

Keywords: Nuclear forces, renormalization group methods, similarity renormalization group, low-resolution potentials, first-principles nuclear theory

Nomenclature

EFT	effective field theory
QCD	quantum chromodynamics
RG	renormalization group
SRG	similarity renormalization group

Key points

- Hamiltonians often have significant off-diagonal matrix elements that make them nonperturbative and difficult to solve.
- Renormalization group methods transform Hamiltonians to lower resolution, replacing explicit, complicated short-distance physics with effective low-energy operators. Such low-resolution potentials are more perturbative and easier to solve.
- The similarity renormalization group generates a continuous unitary transformation, which may be tailored to drive the Hamiltonian towards a diagonal form.
- The similarity renormalization group applied to nuclear forces systematically generates low-resolution potentials that are unitarily equivalent to the original Hamiltonians. The transformation also induces three-body and higher-body forces, which must be treated to achieve exact renormalization group invariance in observables.
- Low-resolution nuclear potentials have driven progress in first-principles nuclear theory due to their perturbativeness and fast convergence behavior.

1 Introduction

Modern nuclear theory has been defined by our developing understanding of theoretical resolution and how to exploit it in studies of nuclear forces, atomic nuclei, and nuclear matter. At its core, theoretical resolution is a choice we make about what to do with high-energy, short-wavelength physics. This short-wavelength or short-range physics may be complicated, difficult to compute, and potentially completely unnecessary to treat explicitly in describing a phenomenon of interest, for example, a nuclear ground state or low-energy scattering. Working at the appropriate resolution means only essential low-energy, long-wavelength physics is included explicitly while the remaining unresolved short-range physics is captured effectively.

While this concept may seem intuitively simple, its application is not always straightforward. Shifting to lower theoretical resolution often requires switching to effective low-energy degrees of freedom and determining unknown effective low-energy interactions. Effective field theories (EFTs) [1–4] and renormalization group (RG) techniques [5, 6] provide systematic ways to construct Hamiltonians at a specific resolution. Both methods have been broadly successful in many domains of physics, and together they have spurred tremendous progress in nuclear theory in the past 25 years. EFTs allow us to construct a low-resolution theory with effective degrees of freedom that is systematically rooted in a higher-resolution underlying theory. Renormalization group methods, on the other hand, allow us to adjust the resolution by integrating out or decoupling irrelevant short-range physics. These methods work well together: We can use an EFT to build a Hamiltonian at a specific resolution and then use RG methods to further tune the resolution of the Hamiltonian, if necessary.

This chapter focuses on the similarity renormalization group (SRG) [7–9]. The SRG is a remarkably simple approach: It is an operator differential equation to compute a unitary transformation of the Hamiltonian, typically used to evolve the Hamiltonian into a more diagonal

2 Similarity renormalization group for nuclear forces

form. In its simplicity, it provides a lot of flexibility, and the SRG has been used to develop low-resolution Hamiltonians and also to solve the quantum many-body problem in fields ranging from cold atoms to quantum chemistry to nuclear physics. Here, we focus on using the SRG to construct low-resolution nuclear forces. We start by revisiting the concept of resolution in detail and making the benefit of low-resolution Hamiltonians clear. The next section introduces the similarity renormalization group, exploring how the RG transformation works and how it impacts the structure of the Hamiltonian. After this, we focus on the application of the SRG to nuclear forces, discussing some key lessons learned over the past 20 years and some challenges that are not yet fully addressed. The last section highlights the progress in computations of nuclei made possible by the SRG and low-resolution Hamiltonians.

2 Physics at low resolution and the renormalization group

In the modern world, resolution is often understood as digital resolution, the density of pixels in an image, which determines the minimum scale of details that image can capture. In physics, one often also thinks about experimental resolution, which is determined not only by the resolution of the instruments one is using, but also by the energy at which the system is probed. High-energy probes have a shorter de Broglie wavelength, which in turn allows them to resolve finer details. Theoretical resolution is analogous: A state $|n\rangle$ with energy E_n resolves interactions with characteristic momentum scales Q with kinetic energies $Q^2/M \lesssim E_n$. Getting the microscopic description of such interactions right is important to correctly model the state $|n\rangle$.

Conversely, it is intuitive to think that modeling a low-energy state, for example, the ground state $|\psi\rangle$ with energy E_{gs} , does not resolve interactions with $Q^2/M > E_{\text{gs}}$. It is easy to see that this is not necessarily the case: If one considers the expansion of the ground-state energy in perturbation theory with the unperturbed Hamiltonian H_0 with eigenstates $|n\rangle$ and the perturbation H_1 , the second-order correction is

$$E^{(2)} = \sum_{n \neq 0} \frac{|\langle 0|H_1|n\rangle|^2}{E_0 - E_n}. \quad (1)$$

Clearly, there is an unrestricted sum over virtual states $|n\rangle$, including many with $E_n \gg E_0 \sim E_{\text{gs}}$. Whether these high-energy states give significant contributions to the ground-state energy depends on the magnitudes of the matrix elements $\langle 0|H_1|n\rangle$ relative to those of the energy differences $E_0 - E_n$. In other words, if H_1 has strong couplings between $|0\rangle$ and $|n\rangle$ for $E_n \gg E_0$, those virtual states are important. Accordingly, the description of the ground state actually requires higher resolution than one might expect. On the other hand, if high-energy states $|n\rangle$ are decoupled from $|0\rangle$, meaning the matrix elements $\langle 0|H_1|n\rangle$ are small, the sum in Eq. (1) may be truncated at small n . This means the ground state can be expanded in low-energy states $|n\rangle$ with E_n less than some energy scale Λ , which is the intrinsic resolution scale of the Hamiltonian H_1 .

Thinking from the perspective of theoretically predicting low-energy phenomena, we can clearly see two very distinct scenarios. When the Hamiltonian resolution scale Λ is large compared to the typical momentum scale Q , our states will be very complicated, with significant contributions from high-energy virtual states. The second-order correction in Eq. (1) will need to be evaluated in a large basis. Moreover, higher-order corrections in perturbation theory will also be significant, and, in general, perturbation theory will diverge and fail, meaning we need to employ nonperturbative approaches. If instead Λ is comparable to Q , things are much simpler. A small basis of a few $|n\rangle$ is sufficient to converge Eq. (1), and perturbation theory is better behaved. Clearly, if possible, we would prefer a lower resolution scale.

So what actually determines the resolution scale Λ ? The answer is: We choose the resolution scale, either implicitly or explicitly. First, we choose the degrees of freedom we use to describe a system. For strong-interaction systems, for example, the fundamental degrees of freedom are quarks and gluons, and their interactions are given by quantum chromodynamics (QCD). In nuclei, however, all quarks are confined in colorless protons and neutrons, so nucleons are more appropriate degrees of freedom. In this case, the complicated dynamics of QCD are replaced by effective nuclear forces between nucleons. What are these nuclear forces? Again, we make a choice here. We can use phenomenological models, as was popular in the previous century, or instead we can use effective field theories and renormalization group techniques to systematically construct nuclear Hamiltonians at a specific resolution.

The freedom to choose the appropriate degrees of freedom and the appropriate (effective) interactions, recasting intractable high-resolution theories into tractable low-energy effective theories, has been essential for progress in theoretical physics. The renormalization group in particular has played a key role in understanding and systematizing the development of effective theories. Many different variants of RG methods exist, but all share some common features:

1. The RG transformation systematically reduces the resolution scale, integrating out high-energy states and degrees of freedom or decoupling them from those relevant at the low-energy scale of interest. Transforming to lower resolution replaces explicit short-range interactions with effective low-energy interactions and short-range degrees of freedom with collective degrees of freedom.
2. Low-energy observables must be preserved, meaning that the short-distance physics that has been decoupled must be replaced with effective low-energy operators. These are resolution dependent (often also referred to as scale dependent) and change continuously as the RG transformation is performed. Renormalization group invariance (or at least approximate invariance) of low-energy observables is a key diagnostic of the method.
3. RG transformations to low resolution also induce many-body interactions. Many-body interactions are natural in effective theories with composite low-energy degrees of freedom (for example, three-body forces when modeling the sun-Earth-moon system using point-like masses). RG transformations show that the division between two-, three-, and higher-body forces is resolution dependent.
4. Crucially, RG transformations to lower resolution also change the physics interpretation. Explicit short-range interactions at high resolution are supplanted by effective low-energy interactions (often with many-body contributions) [10]. Both theoretical models are

valid descriptions of the physics, just at different resolutions, and the low-resolution description is often simpler. Let us illustrate some of these concepts using Eq. (1) as an example again. We have a Hamiltonian

$$H = H_0 + H_1^\Lambda. \quad (2)$$

H_0 is the unperturbed Hamiltonian. It has eigenstates $|n\rangle$ with eigenvalues E_n . H_1^Λ is the perturbation, where we are explicit about the resolution scale Λ . Up to second order in perturbation theory, our prediction for the ground-state energy is

$$E^{(0)} = E_0, \quad E^{(1)}(\Lambda) = \langle 0|H_1^\Lambda|0\rangle, \quad E^{(2)}(\Lambda) = \sum_{\substack{n \neq 0 \\ E_n \leq \Lambda}} \frac{|\langle 0|H_1^\Lambda|n\rangle|^2}{E_0 - E_n}. \quad (3)$$

We are explicit that the first- and second-order energy corrections $E^{(1)}(\Lambda)$ and $E^{(2)}(\Lambda)$ depend on the resolution scale Λ and that the sum over virtual states is already cut off to only include states $|n\rangle$ with $E_n \leq \Lambda$.

Our goal is to determine $H_1^{\Lambda'}$ for $\Lambda' < \Lambda$ such that

$$E^{(1)}(\Lambda') + E^{(2)}(\Lambda') \approx E^{(1)}(\Lambda) + E^{(2)}(\Lambda). \quad (4)$$

Note that we do not expect $E^{(1)}(\Lambda') = E^{(1)}(\Lambda)$ and $E^{(2)}(\Lambda') = E^{(2)}(\Lambda)$ separately. Also, the matching in Eq. (4) does not need to be exact, especially since we are working with a truncated perturbative expansion of the ground state. Pragmatically, it just needs to be within the precision of the original theory for H_1^Λ .

We write $H_1^{\Lambda'} = H_1^\Lambda + \delta H_1$ and consider the case $\Lambda' = \Lambda - \delta\Lambda$ where $\delta\Lambda$ is small. We may assume δH_1 is small and neglect terms that are quadratic in δH_1 . In this case, Eq. (4) simplifies to

$$\sum_{\substack{n \neq 0 \\ \Lambda' < E_n \leq \Lambda}} \frac{|\langle 0|H_1^\Lambda|n\rangle|^2}{E_0 - E_n} \approx \langle 0|\delta H_1|0\rangle + \sum_{\substack{n \neq 0 \\ E_n \leq \Lambda'}} \frac{\langle 0|H_1^\Lambda|n\rangle \langle n|\delta H_1|0\rangle}{E_0 - E_n}. \quad (5)$$

To progress further, we would need to be more specific about the Hamiltonian and the RG approach to determine the form of δH_1 . Still, we clearly see the decoupled parts of H_1^Λ from Λ' to Λ on the left-hand side. These must be effectively captured by new interactions δH_1 on the right-hand side. This ensures renormalization group invariance of the total ground-state energy $E_{\text{gs}} \approx E^{(0)} + E^{(1)} + E^{(2)}$. The resulting δH_1 contributes at both first and second order in perturbation theory and together these compensate for the decoupled parts of H_1^Λ . In particular the nonzero first-order contribution $\langle 0|\delta H_1|0\rangle$ shows that the decoupled high-energy physics is now shuffled into low-energy effective operators. Changing resolution also changes the split of contributions between first, second, and higher orders in perturbation theory.

Additionally, if we suppose H_1^Λ and $H_1^{\Lambda'}$ are two-body interactions, we can consider computations of the three-body system using both Hamiltonians. What one will observe is that H_1^Λ and $H_1^{\Lambda'}$ give different three-body binding energies, especially for Λ' significantly smaller than Λ . This shows that the effective two-body interaction δH_1 induced through the RG transformation does not on its own guarantee RG invariance of the three-body binding energy and an induced three-body force is required. Demanding exact RG invariance for the four-body, five-body, and higher-body systems will show that also four-body, five-body, and many-body forces are induced. How large these are and whether they really need to be accounted for can be studied by looking at the resolution scale dependence of many-body observables, like binding energies, densities, excitation spectra, and so on.

The example in this section is admittedly schematic, but it illustrates many of the key features of the renormalization group, in particular how high-energy physics in the Hamiltonian is decoupled and how it is captured by new effective interactions. Many renormalization group methods exist, which primarily differ in how the decoupling is performed, how the effective interaction is constructed, and how RG invariance is enforced. Below we discuss the similarity renormalization group, which has emerged as a popular RG variant in nuclear physics mostly due to its robustness and broad applicability.

3 The similarity renormalization group

The similarity renormalization group was first presented by Głazek, Wilson, and Wegner in 1994 [7, 8] and introduced to nuclear physics over a decade later [9]. The original publications focused on the renormalization of Hamiltonians in relativistic field theories [7] and condensed matter systems [8]. In both cases, strong off-diagonal couplings between low- and high-energy states in the Hamiltonians made them nonperturbative and difficult to solve, and the common approach developed was a continuous unitary renormalization group transformation to suppress off-diagonal matrix elements and bring the Hamiltonian closer to diagonalization. We discuss this approach in this section and the application to nuclear forces in the next.

Starting from any Hamiltonian H , we want to perform a unitary similarity transformation

$$H(s) = U(s) H U^\dagger(s). \quad (6)$$

The transformation is a function of a continuous flow parameter s , and $s = 0$ is the initial condition with $U(0) = 1$. Note that this is an

4 Similarity renormalization group for nuclear forces

operator equation, valid in any basis. Differentiating with respect to s gives the flow equation

$$\frac{dH(s)}{ds} = [\eta(s), H(s)] \quad (7)$$

with the generator $\eta(s)$ and the commutator $[A, B] = AB - BA$. The SRG unitary transformation is performed by solving the coupled differential equation (7) from $s = 0$ towards $s \rightarrow \infty$.

The anti-Hermitian generator

$$\eta(s) = U(s) \frac{dU^\dagger(s)}{ds} \quad (8)$$

determines the SRG unitary transformation. So how do we choose an appropriate generator? Many equivalent choices are possible, and it is instructive to consider the ansatz proposed by Wegner. We split the Hamiltonian into diagonal and off-diagonal parts¹

$$H = H_d + H_{od}. \quad (9)$$

We ignore the dependence on the flow parameter s , but in general H_d and H_{od} are s -dependent. Wegner suggested the generator

$$\eta = [H_d, H] = [H_d, H_{od}]. \quad (10)$$

The matrix representation of H_d is just $\varepsilon_i \delta_{ij}$ with the diagonal matrix elements $\varepsilon_i = H_{ii}$. With this, Eq. (10) simplifies to

$$\eta_{ij} = H_{ij}(\varepsilon_i - \varepsilon_j). \quad (11)$$

We see that the matrix elements η_{ij} vanish if the off-diagonal matrix elements H_{ij} ($i \neq j$) vanish. In this case, the SRG flow equation (7) has reached a fixed point where the decoupling condition, i.e., the full diagonalization of the Hamiltonian, is met.² The generator matrix elements are proportional to the energy difference $\varepsilon_i - \varepsilon_j$. As we see below, this is responsible for decoupling states i and j based on their energy differences.

Plugging Eq. (11) into the flow equation (7), we get

$$\frac{dH_{ij}}{ds} = [\eta, H]_{ij} = -(\varepsilon_i - \varepsilon_j)^2 H_{od,ij} + \sum_k (\varepsilon_i + \varepsilon_j - 2\varepsilon_k) H_{od,ik} H_{od,kj}. \quad (12)$$

To gain more insight into what is going on, we consider on a perturbative analysis where we assume $H_d \gg H_{od}$. This is a reasonable starting point, but of course the degree to which this assumption is met depends on the specifics of the system and problem at hand. Under this assumption, the first term on the right hand-side proportional to $(\varepsilon_i - \varepsilon_j)^2$ dominates. This only changes off-diagonal matrix elements, and if we neglect the second term we can perform the integration to find

$$H_{ij}(s) = H_{ij}(0) \exp[-(\varepsilon_i - \varepsilon_j)^2 s], \quad (i \neq j). \quad (13)$$

In this approximation the diagonal matrix elements ε_i are independent of s . We see that the off-diagonal matrix elements are suppressed as s grows. How strongly they are suppressed depends on the energy difference $\varepsilon_i - \varepsilon_j$. From this, we see that we do not need to integrate all the way to $s \rightarrow \infty$; it is good enough to integrate to an s where the problematic large off-diagonal matrix elements have been driven to 0 and the remaining Hamiltonian can be solved. If we do everything exactly, $H(s)$ at any s is unitarily equivalent to $H(0)$, giving the same results for observables.

Clearly the generator defined by Wegner is doing what we want, which is suppressing off-diagonal matrix elements and driving the Hamiltonian towards the diagonal. Other choices for the generator are also possible, and we discuss an alternative that has proliferated in nuclear physics in the next section. In general, researchers have explored generators of the form

$$\eta(s) = [G(s), H(s)], \quad (14)$$

where one has to choose the Hermitian matrix $G(s)$. Picking $G(s)$ to have the form you want to drive the Hamiltonian towards (for example, band diagonal or block diagonal) has proven to be an effective ansatz to achieve the desired decoupling [11].

The SRG induces many-body interactions, even if the starting Hamiltonian only contains one- and two-body interactions. To see this we use second quantization to express our Hamiltonian in terms of creation operators a_i^\dagger and annihilation operators a_i (with $a_i^\dagger |0\rangle = |i\rangle$):

$$H = T + V = \sum_{ij} t_{ij} a_i^\dagger a_j + \frac{1}{4} \sum_{ijkl} v_{ijkl} a_i^\dagger a_j^\dagger a_l a_k. \quad (15)$$

The one-body operator T (for example, the kinetic energy or an external potential) is expressed in terms of its matrix elements t_{ij} , which parametrizes interactions between particles in the single-particle states $|i\rangle$ and $|j\rangle$. Similarly, the two-body operator V with matrix elements

¹The definition of “diagonal” and “off-diagonal” parts is arbitrary, but one typically chooses a convenient basis where the diagonal part is simply the diagonal matrix elements of the Hamiltonian.

²Note that using the SRG to perform a full diagonalization is neither efficient nor numerically stable because the flow equation becomes increasingly stiff as the Hamiltonian reaches a diagonal form. In general, the SRG is used to evolve Hamiltonians towards a band-diagonal form, where matrix elements outside a band around the diagonal have all been driven to 0. Band-diagonal Hamiltonians with sufficiently narrow bands have localized eigenstates, making them easier to solve.

v_{ijkl} generates interactions between pairs of particles, for example, taking particles from the states $|k\rangle, |l\rangle$ to $|i\rangle, |j\rangle$. The generator also has one- and two-body parts:

$$\eta = \sum_{ij} \eta_{ij} a_i^\dagger a_j + \frac{1}{4} \sum_{ijkl} \eta_{ijkl} a_i^\dagger a_j^\dagger a_l a_k. \quad (16)$$

Evaluating the commutator in Eq. (7) gives expressions of the form

$$[a_i^\dagger a_j^\dagger a_l a_k, a_a^\dagger a_b^\dagger a_d a_c] = a_i^\dagger a_j^\dagger a_l a_k a_a^\dagger a_b^\dagger a_d a_c - a_a^\dagger a_b^\dagger a_d a_c a_i^\dagger a_j^\dagger a_l a_k. \quad (17)$$

Each of the terms on the right-hand side must be simplified using normal ordering techniques, and after some work one finds that there are terms proportional to $a_p^\dagger a_q^\dagger a_r^\dagger a_u a_t a_s$ and $a_p^\dagger a_q^\dagger a_r^\dagger a_s a_w a_u a_t$, which are three- and four-body operators, respectively. The subtraction in Eq. (17) causes the four-body operators to cancel exactly, but the three-body operators remain. These are induced three-body interactions generated by the SRG transformation, and further iteration introduces many-body forces.

If we are only interested in two-body systems, three-body interactions do not contribute so we do not need to care and can solve the SRG equations in the two-body Hilbert space. However, if we look at three-body systems, for the SRG transformation to be perfectly unitary, which means leaving all eigenvalues and observables unchanged, we need to solve the SRG equations in the three-body Hilbert space. Doing this allows us to capture the induced three-body interactions, which are essential to guarantee exact renormalization group invariance as s goes from 0 towards ∞ . Four-body interactions are also induced, and capturing these would require evaluating the SRG equations in the four-body Hilbert space. Solving the SRG equations in the four-body Hilbert space and beyond is currently impractical, so induced many-body interactions beyond three-body forces are not accounted for. The size of these interactions can be probed by checking RG invariance: How much does a prediction for an observable depend on the value of s ? Ideally, we find that varying s only changes predicted observables a little,³ which indicates that missing induced many-body interactions are small.

4 Generating low-resolution nuclear forces

Nuclear forces have been traditionally thought of as nonperturbative, with a hard repulsive core required to give nuclear saturation [12–15]. This hard core strongly couples low- and high-energy states, preventing any perturbative description of nuclei. The renormalization group tells us that this picture is more complicated than necessary. Such hard core potentials are one possible paradigm for nuclear forces, but other lower-resolution theories and models are also possible. In particular, modern potentials from chiral and pionless effective field theory may be constructed at lower resolution, making them more perturbative and easier to solve in many-body calculations. The SRG allows us to further transform nuclear Hamiltonians (from effective field theory, phenomenological fits, or other methods) to even lower resolution, making them even more perturbative.

Nuclear Hamiltonians generally have the form

$$H = T - T_{\text{cm}} + V_{\text{NN}} + V_{3\text{N}}. \quad (18)$$

We have the intrinsic kinetic energy $T - T_{\text{cm}}$ with the center of mass subtracted (often also called T_{int} or T_{rel}), a nucleon-nucleon potential V_{NN} , and a three-nucleon potential $V_{3\text{N}}$. We are neglecting four-nucleon interactions, which exist and are for example predicted at next-to-next-to-next-to-leading order in chiral effective field theory [2, 3].

In this section, we focus on the SRG for nucleon-nucleon forces and only briefly discuss the application to three-nucleon forces [16, 17]. Nucleon-nucleon forces may be represented in a Jacobi plane-wave partial-wave basis

$$|p(LS)JM_J T M_T\rangle \equiv |p \alpha_{\text{NN}}\rangle. \quad (19)$$

$p = |\mathbf{p}|$ is the magnitude of the Jacobi momentum $\mathbf{p} = (\mathbf{k}_1 - \mathbf{k}_2)/2$, where \mathbf{k}_1 and \mathbf{k}_2 are the momenta of the first and second nucleon, respectively. The isospin and angular momentum dependence of the potential is captured in the partial-wave quantum numbers α_{NN} : the relative orbital angular momentum L , the total two-body spin S , the coupled angular momentum J with its projection M_J , and the two-body isospin T with its projection M_T . For simplicity, we focus on singlet channels, where $S = 0$, where the potential is diagonal in all

³How much or little ultimately depends on the precision of our theory. If we are using a leading order effective theory with uncertainties of $\sim 30\%$, it may be acceptable to have significant, but controlled dependence on s within this uncertainty.

6 Similarity renormalization group for nuclear forces

partial-wave quantum numbers.⁴ In this case, we can write nucleon-nucleon potentials simply as

$$V(p', p) = \langle p' \alpha_{\text{NN}} | V_{\text{NN}} | p \alpha_{\text{NN}} \rangle. \quad (22)$$

In nuclear physics, choosing the generator as

$$\eta(s) = [T_{\text{rel}}, H(s)] \quad (23)$$

has emerged as a standard choice [18, 19]. This follows the established intuition for the SRG that, since T_{rel} is diagonal in the plane-wave partial-wave basis, choosing $G = T_{\text{rel}}$ in Eq. (14) will drive $H(s)$ towards the diagonal. Plugging all of this into the SRG flow equation gives:⁵

$$\frac{dV_s(p', p)}{ds} = -(p'^2 - p^2)^2 V_s(p', p) + \frac{2}{\pi} \int_0^\infty q^2 dq (p^2 + p'^2 - 2q^2) V_s(p, q) V_s(q, p'). \quad (25)$$

Assuming $T_{\text{rel}} \gg V_s$, we see that the first term dominates, giving

$$V_s(p', p) = V_{s=0}(p', p) \exp[-(p'^2 - p^2)^2 s]. \quad (26)$$

off-diagonal matrix elements are suppressed based on the kinetic energy difference $p'^2 - p^2$. Changing variables to

$$\lambda = \frac{1}{s^{1/4}}, \quad (27)$$

where λ has units of fm^{-1} , helps us to further analyze the behavior of the SRG equation. Now the SRG equations are instead integrated from $\lambda = \infty$ towards $\lambda = 0$, and

$$V_\lambda(p', p) = V_\infty(p', p) \exp[-(p'^2 - p^2)^2 / \lambda^4]. \quad (28)$$

This change of variables is useful because λ has the clear interpretation of a resolution scale that is lowered by the SRG transformation as we integrate towards $\lambda = 0 \text{ fm}^{-1}$, and off-diagonal matrix elements outside of a band of width λ^2 are exponentially suppressed.

For nucleon-nucleon potentials, solving the SRG is simple. Equation (25) can be solved on a laptop using established adaptive differential equation solvers. Accompanying this chapter is a Python code `nn-srg` [20, 21] to allow readers to experiment with the SRG transformation of nucleon-nucleon potentials. Let us now turn our attention to the SRG in practice.

Low-resolution nucleon-nucleon potentials

In Fig. 1, we visualize the evolution of nuclear potentials as they are transformed to lower resolution using the SRG. Each panel shows $V(p', p)$ in the neutron-proton 1S_0 channel with p', p up to 5 fm^{-1} . The leftmost panel is the untransformed potential (as originally constructed from the effective field theory or phenomenological methods). Going to the right, we transform the potential using the SRG to lower resolution scales λ all the way down to $\lambda = 1.8 \text{ fm}^{-1}$. The top row considers the EM500 potential [22], constructed at next-to-next-to-next-to-leading order in chiral effective field theory. Looking at the initial potential on the left, we see that matrix elements with $p', p \gtrsim 3.2 \text{ fm}^{-1}$ are approximately 0. This is due to the $\Lambda = 500 \text{ MeV} \approx 2.5 \text{ fm}^{-1}$ cutoff used in the construction of the EM500 potential, which sets its resolution scale. The SRG transformation to lower resolutions initially does very little. $\lambda = 4.0 \text{ fm}^{-1}$ and $\lambda = \infty$ are nearly identical. Once $\lambda \leq \Lambda$ the off-diagonal matrix elements begin to be suppressed, and the SRG transformation drives the potential towards a band-diagonal form as desired. At $\lambda = 1.8 \text{ fm}^{-1}$, all matrix elements $V(0, p)$ with $p > 1.8 \text{ fm}^{-1}$ are strongly suppressed, so low- and high-momentum degrees of freedom have been successfully decoupled. In Fig. 2, we see that this suppression of off-diagonal matrix elements is exponential as predicted by Eq. (28).

For comparison, we also show a phenomenological nucleon-nucleon potential, AV18, in the bottom row of Fig. 1 [14]. AV18 has a hard repulsive core, which leads to strong coupling between low and high momenta. Clearly the matrix elements $V_\infty(0, p)$ are sizable up to and beyond $p = 5 \text{ fm}^{-1}$. The AV18 potential has an intrinsically high resolution. This is due to its construction and its optimization to nucleon-nucleon scattering at relatively high energies. Nonetheless, the SRG transformation systematically drives the potential to a diagonal form,

⁴Symmetries of nuclear forces require that all nucleon-nucleon partial-wave quantum numbers are diagonal except L , which is $J \pm 1$ in coupled channels where $S = 1$. To generalize the expressions for singlet channels, replace integrals over intermediate momenta

$$\frac{2}{\pi} \int q^2 dq \quad (20)$$

with an additional sum over possible intermediate channels

$$\frac{2}{\pi} \sum_\alpha \int q^2 dq. \quad (21)$$

⁵We use the normalization

$$1 = \frac{2}{\pi} \int_0^\infty q^2 dq |q\rangle \langle q|. \quad (24)$$

We use units such that $\hbar c = 1$ and the nucleon mass $M_N = 1$. T_{rel} then has matrix elements $T_{\text{rel}}(p', p) = p^2 \frac{\pi}{2} \frac{\delta(p-p')}{pp'}$.

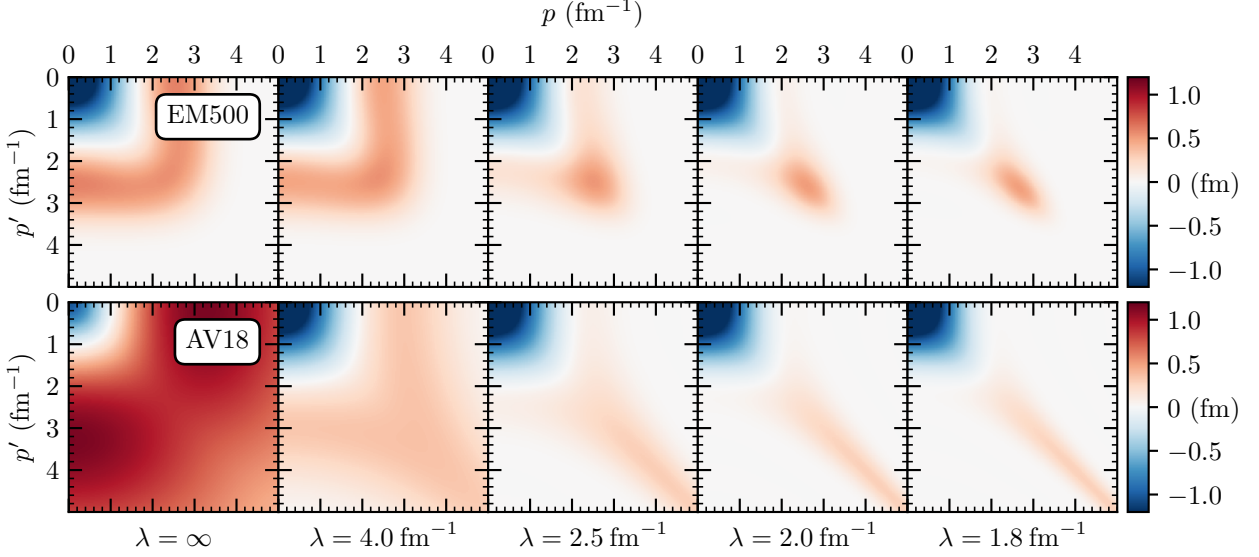


Fig. 1 Jacobi momentum-space nucleon-nucleon potential matrix elements $V(p', p)$ in the neutron-proton 1S_0 channel for various Hamiltonians. We consider two initial Hamiltonians: the “EM500” nucleon-nucleon potential (top) from chiral effective field theory at next-to-next-to-next-to-leading order [22]; and the phenomenological “AV18” nucleon-nucleon potential (bottom) [14]. Due to its repulsive short-range core, AV18 clearly couples low and high momenta strongly with nonzero matrix elements $V(0, p)$ beyond $p = 5 \text{ fm}^{-1}$. On the other hand, the $\Lambda = 500 \text{ MeV}$ cutoff of the EM500 potential regularizes high-momentum behavior such that matrix elements with $p, p' \gtrsim 3.2 \text{ fm}^{-1}$ are approximately 0. For both potentials, we show the SRG transformation to lower resolution scales λ , down to $\lambda = 1.8 \text{ fm}^{-1}$. We see that the potentials are driven towards a band-diagonal form, and matrix elements $V(0, p)$ with $p > \lambda$ are suppressed. Once SRG transformed to low resolution, AV18 and EM500 have very similar low-momentum matrix elements.

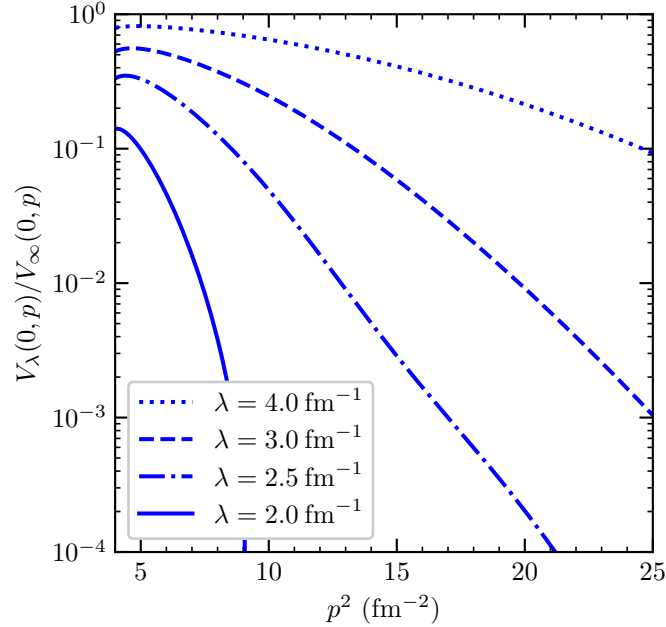


Fig. 2 Matrix element suppression for the matrix elements $V_\lambda(0, p)$ visualized through the ratio $V_\lambda(0, p)/V_\infty(0, p)$. The initial Hamiltonian is the EM500 potential in the neutron-proton 1S_0 channel. As the EM500 potential is SRG transformed to lower resolution scales λ , the off-diagonal matrix elements with $p > \lambda$ are exponentially suppressed as predicted in Eq. (28).

successfully decoupling low and high momenta in the low-resolution potential. At $\lambda = 1.8 \text{ fm}^{-1}$, the low-resolution potentials obtained from the EM500 and AV18 potentials at $\lambda = \infty$ have very similar low-momentum matrix elements. This is because they both accurately

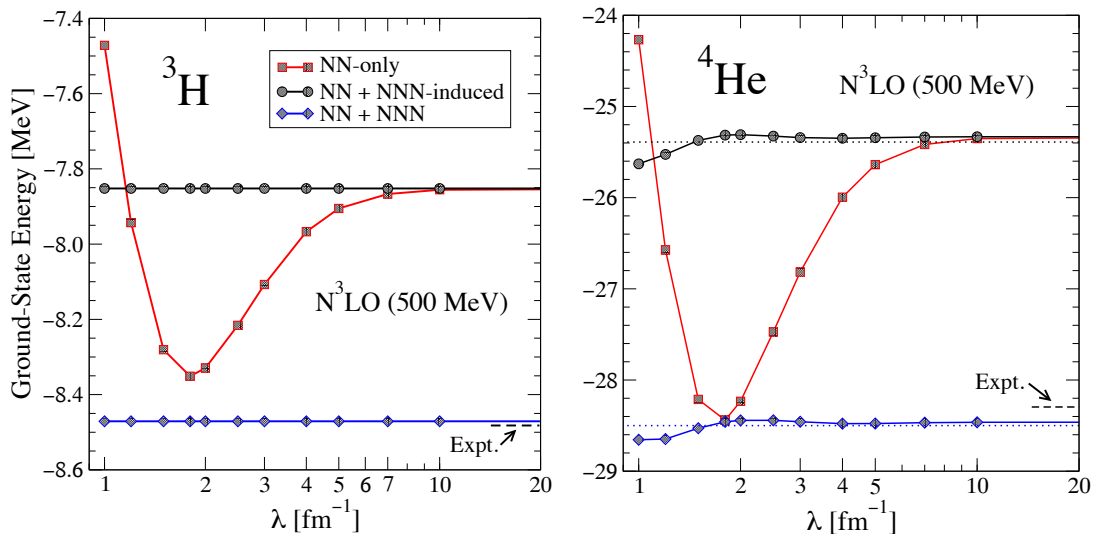


Fig. 3 The ground-state energies of ^3H (left) and ^4He (right) computed with nuclear Hamiltonians from chiral effective field theory that have been transformed using the similarity renormalization group to lower resolution scales λ . We compare the behavior of the ground-state energy for various λ when only SRG-evolved nucleon-nucleon potentials are used (NN-only, black line), when the SRG-induced three-nucleon interactions are included (NN + NNN-induced, red line), and when a three-nucleon potential is included in the initial Hamiltonian (NN + NNN, blue line). For ^3H , accounting for induced three-nucleon interactions is required for SRG invariance of the ground-state energy, and the inclusion of explicit three-nucleon forces is required to reproduce the experimental value. For $\lambda \geq 1.8 \text{ fm}^{-1}$, the predicted ground-state energy of ^4He is approximately independent of λ , indicating that induced four-body forces are small. Figure adapted from [16].

reproduce low-energy nucleon-nucleon scattering phase shifts (which are not affected by the SRG transformation) and so the low-resolution potentials “collapse” to universal forms [6, 23–25].

Induced many-body forces

We now clearly see how the SRG transforms nuclear forces to lower resolution. This transformation is unitary, and it leaves nucleon-nucleon observables and nucleon-nucleon phase shifts unchanged while decoupling low- and high-momentum degrees of freedom. As we know, RG transformations induce many-body interactions, and the SRG is no exception. In the left panel of Fig. 3, we see this for the ^3H ground-state energy. When only the nucleon-nucleon interactions are transformed using the SRG (NN-only), the ground-state energy is not invariant as a function of λ . This is due to missing induced three-body interactions.

Consistently performing the SRG transformation for two- and three-nucleon forces is challenging but possible. In general, one needs to perform the SRG transformation for the two- and three-body Hamiltonians at the same time:

$$H_2(s) = U(s)(T_{\text{rel}} + V_{\text{NN}})U^\dagger(s), \quad (29)$$

$$H_3(s) = U(s)(T_{\text{rel}} + V_{\text{NN}} + V_{3\text{N}})U^\dagger(s). \quad (30)$$

At every s , one can unambiguously identify the new nucleon-nucleon and three-nucleon potentials sequentially:

$$V_{\text{NN}}(s) = H_2(s) - T_{\text{rel}}, \quad (31)$$

$$V_{3\text{N}}(s) = H_3(s) - T_{\text{rel}} - V_{\text{NN}}(s). \quad (32)$$

If we include no initial three-nucleon forces [i.e., $V_{3\text{N}}(s=0) = 0$], the induced three-nucleon potential $V_{3\text{N}}(s)$ ensures that, for example, the ^3H ground-state energy is invariant under the SRG transformation (see NN + NNN-induced in Fig. 3). Three-nucleon forces are always present and are essential for an accurate description of nuclei and nuclear matter [26–28]. Including the initial three-nucleon potential in the Hamiltonian in Fig. 3 brings the ^3H ground-state energy into agreement with experiment at $\lambda = \infty$ (see NN + NNN). Moreover, the SRG transformation does not change E_{gs} , indicating that $V_{\text{NN}}(s)$ and $V_{3\text{N}}(s)$ are being transformed consistently to ensure that the full three-body Hamiltonian is unitarily equivalent to the initial Hamiltonian.

Performing the SRG consistently for two- and three-nucleon potentials is the current state-of-the-art in nuclear physics [16, 17, 28, 29]. Both initial and induced four-nucleon forces are neglected. This is not necessarily a problem as the contributions of four-nucleon interactions in nuclei may very well be smaller than other uncertainties in our calculations. Still this uncertainty should be studied and quantified, and we currently rely on variations of the SRG resolution scale λ as a diagnostic of the uncertainty associated with neglected four-body and many-body forces. As one example, we see the impact of missing induced four-nucleon forces in calculations of the ground-state energy

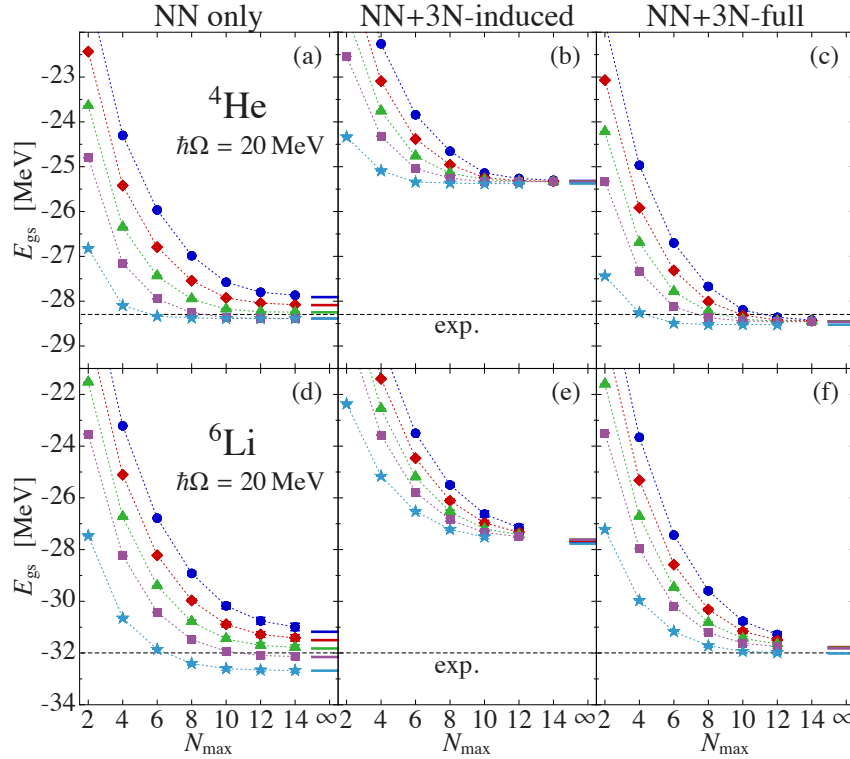


Fig. 4 Ground-state energies of ${}^4\text{He}$ (top) and ${}^6\text{Li}$ (bottom) computed with the no-core shell model using Hamiltonians from chiral effective field theory that have been transformed to lower resolution scales λ . The SRG scales are $\lambda = 2.2 \text{ fm}^{-1}$ (dark blue circles), 2.1 fm^{-1} (red diamonds), 2.0 fm^{-1} (green triangles), 1.9 fm^{-1} (purple squares), and 1.6 fm^{-1} (teal stars). In no-core shell model calculations, the Hamiltonian is expanded in a basis truncated based on the parameter N_{max} . The ground-state energies are shown as a function of N_{max} , where the extrapolation to $N_{\text{max}} \rightarrow \infty$ is indicated on the very right. As in Fig. 3, we consider cases where only the nucleon-nucleon force has been SRG transformed (NN only), where the SRG-induced three-nucleon interactions are accounted for (NN+3N-induced), and where the Hamiltonian also includes an initial three-nucleon force before the SRG transformation (NN+3N-full). As in Fig. 3, consistently transforming both two- and three-nucleon potentials is required to achieve SRG invariance and the inclusion of the the initial three-nucleon force is important for agreement with experiment. Comparing $\lambda = 2.2 \text{ fm}^{-1}$ and 1.6 fm^{-1} (dark blue circles and teal stars, respectively), the ground-state energy converges much more quickly in N_{max} for $\lambda = 1.6 \text{ fm}^{-1}$. This improved convergence substantially reduces the computational cost required to deliver converged calculations and makes calculations in heavier nuclei up to around ${}^{16}\text{O}$ possible. Figure from [29].

of ${}^4\text{He}$ in the right panel of Fig. 3. Even with consistent SRG transformation of two- and three-nucleon potentials, the ground-state energy varies weakly as λ is reduced below 3 fm^{-1} and more strongly as λ approaches 1 fm^{-1} . The effect of the induced four-nucleon forces is small overall, and we can conclude that for calculations of ${}^4\text{He}$ neglecting these induced forces is a small, controlled approximation.

The SRG is a mature method in nuclear physics, but induced many-body interactions are still a significant challenge. As we see in the next section, low-resolution forces make calculations of nuclei much easier, reducing computational costs by orders of magnitude. This is especially true for very soft interactions, with $\lambda \lesssim 2.0 \text{ fm}^{-1}$. However, SRG transformations to such low resolution carry the risk of inducing significant four-nucleon interactions. Quantifying the size of these is difficult, so we must tread with caution. Any improvement to how many-body forces are induced in the SRG (for example, by developing a generator that induces smaller many-body forces or by approximately accounting for induced four-nucleon forces via low-resolution fits [30]) would have a significant positive impact on calculations of nuclei.

5 Implications for nuclei

Solving the many-body Schrödinger equation is a challenging task, and for a long time first-principles (or ab initio) calculations based on nuclear forces were limited to light nuclei [31]. Now comprehensive studies of medium-mass nuclei [32–43] and also leadership calculations of heavy [44–50] and even super-heavy isotopes [51] are possible. This advance was driven by two combined efforts: 1) the development of low-resolution nuclear Hamiltonians using effective field theories and renormalization group methods [2–4, 6]; and 2) the development

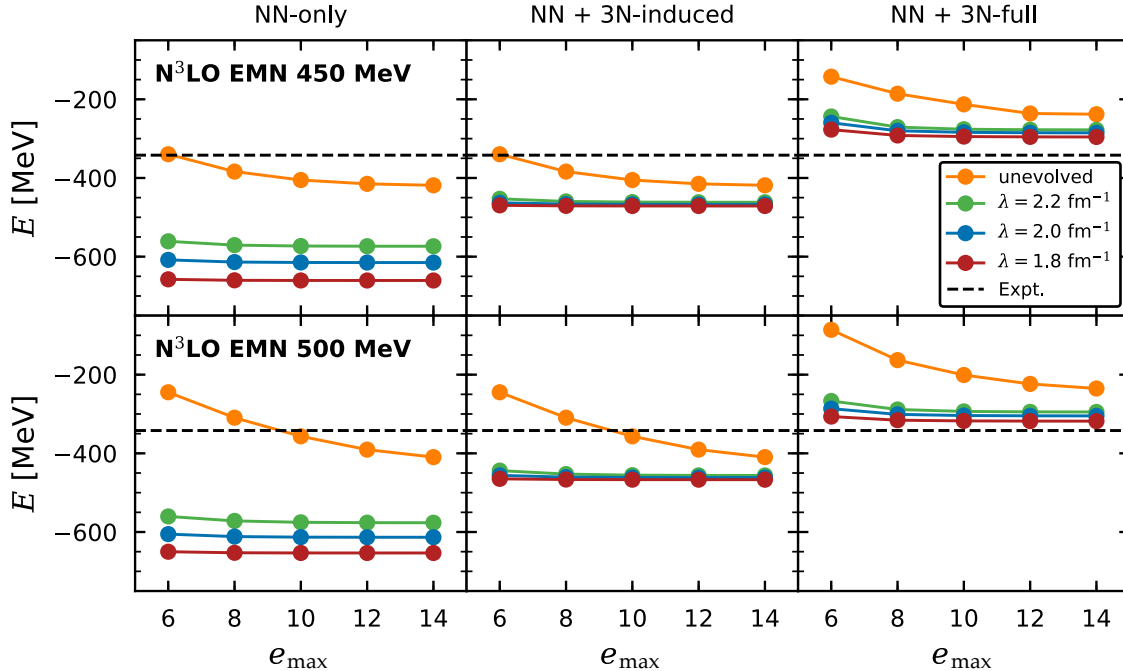


Fig. 5 Ground-state energies of ^{40}Ca computed with the in-medium similarity renormalization group using Hamiltonians from chiral effective field theory that have been transformed to lower resolution scales λ . The SRG scales are unevolved, i.e., $\lambda = \infty$, (orange), 2.2 fm^{-1} (green), 2.0 fm^{-1} (blue), and 1.8 fm^{-1} (red). In in-medium similarity renormalization group calculations, the Hamiltonian is expanded in a single-particle basis truncated based on the parameter e_{max} . As in Fig. 3, we consider cases where only the nucleon-nucleon force has been SRG transformed (NN-only), where the SRG-induced three-nucleon interactions are accounted for (NN + 3N-induced), and where the Hamiltonian also includes an initial three-nucleon force before the SRG transformation (NN + 3N-full). Unevolved Hamiltonians converge slowly in e_{max} in all cases, while SRG-transformed Hamiltonians converge quickly. This improved convergence substantially reduces the computational cost required to deliver converged calculations. Figure adapted from [56].

of scalable many-body methods that solve the Schrödinger equation in an approximate, but systematically improvable way [52–55]. The SRG was a key method in the development of low-resolution Hamiltonians and is now part of the foundation of modern nuclear theory.

The essential role of low-resolution forces in nuclear structure theory cannot be overstated. Many methods to solve the Schrödinger equation rely on basis expansions, which expand nuclear Hamiltonians in a basis of harmonic oscillator wave functions. Their computational costs scale with the size of the basis N , either exponentially $\mathcal{O}(e^N)$ for exact diagonalizations or polynomially, e.g., $\mathcal{O}(N^6)$, for approximate, scalable many-body methods. Low-resolution Hamiltonians have significantly reduced couplings to high-energy states. This accelerates convergence in the basis truncation, ultimately allowing for converged calculations in smaller bases. This is the main benefit of low-resolution forces in calculations of nuclei.

Let us explore two examples of improved convergence in calculations of nuclei. In Fig. 4, we show calculations of the ground-state energies of ^4He and ^6Li using the no-core shell model [29]. The no-core shell model performs an exact diagonalization of the many-body Hamiltonian, where the Hamiltonian is expanded in a basis of A -body states. This basis is truncated based on N_{max} , limiting the maximum number of excitations in a state relative to the lowest energy state (with $N_{\text{max}} = 0$). No-core shell model calculations must take N_{max} large enough to observe that their calculations become independent of this truncation at which point the calculation is converged. The cost of the diagonalization scales exponentially in N_{max} , so reducing the N_{max} required to reach convergence can easily lower the cost of a calculation by orders of magnitude.

First, consider calculations only using nucleon-nucleon interactions (left column, NN only). The different colored points correspond to different SRG resolution scales λ . The dark blue circles are $\lambda = 2.2 \text{ fm}^{-1}$, while the blue stars are $\lambda = 1.6 \text{ fm}^{-1}$. For $\lambda = 2.2 \text{ fm}^{-1}$, the ground-state energy of ^4He is only converged at $N_{\text{max}} = 12$, and that of ^6Li is not converged even at $N_{\text{max}} = 14$ and requires extrapolation to $N_{\text{max}} \rightarrow \infty$. We contrast this with $\lambda = 1.6 \text{ fm}^{-1}$, where converged ground-state energies are obtained for ^4He and ^6Li at $N_{\text{max}} = 6$ and 8 , respectively.

One thing to note here is that the converged results for different lines corresponding to different λ do not agree. This is because induced three-nucleon interactions are not accounted for. In the center and right columns, we see that including induced and initial three-nucleon interactions gives converged predictions that agree between all λ . We also see that the nuclear forces SRG transformed to $\lambda = 1.6 \text{ fm}^{-1}$ still converge much more quickly in N_{max} . The ground-state energy of ^6Li is converged at $N_{\text{max}} = 8$, which is 100–1000 times cheaper to compute than $N_{\text{max}} = 12$, which is still not sufficient to provide a converged result for $\lambda = 2.2 \text{ fm}^{-1}$. The improved convergence and corresponding reduction in cost extends the reach of the no-core shell model, enabling calculations of systems that could not be computed otherwise.

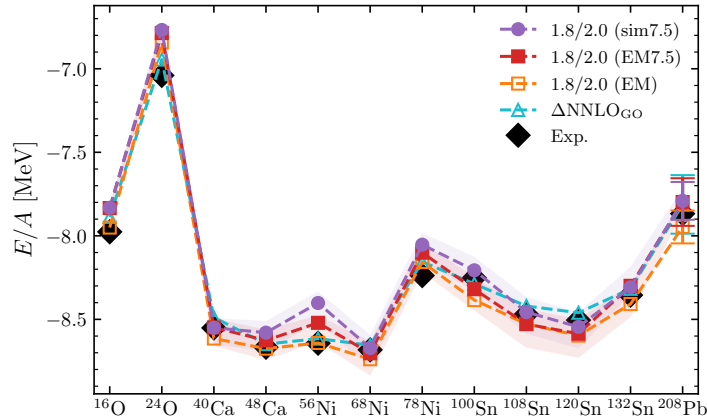


Fig. 6 Ground-state energy per nucleon E/A for selected nuclei computed using low-resolution nuclear Hamiltonians [30, 50, 58]. The 1.8/2.0 (EM), 1.8/2.0 (EM7.5), and 1.8/2.0 (sim7.5) Hamiltonian are constructed using SRG-transformed potentials with $\lambda = 1.8 \text{ fm}^{-1}$. The $\Delta\text{NNLO}_{\text{GO}}$ Hamiltonian is instead explicitly constructed with a low cutoff of $\Lambda = 2.0 \text{ fm}^{-1}$, motivated by the success of SRG-evolved low-resolution Hamiltonians. The agreement with experimental binding energies across the nuclear chart is remarkable. Figure adapted from [50].

In Fig. 5, we consider instead ground-state energies of ^{40}Ca computed using the in-medium similarity renormalization group (IMSRG) [56]. The IMSRG [53, 57] is a many-body method based on the SRG idea of decoupling, but applied to the quantum many-body problem. The IMSRG differs from the SRG in its decoupling strategy; it performs a block diagonalization of the many-body Hamiltonian, starting from a reference state that approximates the ground state of the nucleus of interest and decoupling only that reference state from its excitations. Thus the IMSRG transformation is specific to each system computed (hence the name “in-medium” SRG), which allows the IMSRG to efficiently solve the many-body problem. However, this also prevents it from being used to derive general low-resolution Hamiltonians like the “free-space” SRG discussed in this chapter.

In IMSRG calculations, the Hamiltonian is expanded in a basis of single-particle harmonic oscillator states. This basis is truncated, including only states with a harmonic oscillator energy up to a given value e_{max} . As with the no-core shell model, IMSRG calculations must show that their predictions are sufficiently converged with respect to e_{max} . The IMSRG scales polynomially in the basis size, so calculations with larger e_{max} are not as expensive as similar increases in N_{max} . Still, a calculation with $e_{\text{max}} = 10$ is approximately 20–30 times cheaper than a calculation with $e_{\text{max}} = 14$, making the improved convergence of SRG-transformed Hamiltonians very valuable.

The trends in Fig. 5 are very similar to those in Fig. 4. The SRG-unevolved Hamiltonians (orange) converge slowly in e_{max} , especially when three-nucleon forces are included. The Hamiltonians that have been SRG evolved to lower resolution scales λ (green, blue, and red) all exhibit much faster convergence with respect to e_{max} . $e_{\text{max}} = 10$ is converged in all cases, and when only nucleon-nucleon forces are included even $e_{\text{max}} = 8$ is converged. The results with only nucleon-nucleon forces are of course strongly dependent on λ because induced three-body forces have not been accounted for. Analogous findings also apply to other many-body methods, such as many-body perturbation theory [54], coupled cluster theory [52], and self-consistent Green’s function theory [55], when they are expanded in harmonic oscillator bases.

When low-resolution nuclear forces were introduced, it did not take long for them to lead to many successful applications in calculations of nuclei [59–61]. Over the past 20 years, low-resolution forces have remained very successful, and different approaches to constructing them have proliferated:

- $V_{\text{low } k}$ [23, 24] and the unitary correlation operator method [62, 63] both implemented renormalization group transformations for nucleon-nucleon forces, but faced difficulties with the consistent renormalization group transformations for three-nucleon forces.
- This challenge was solved by the SRG, where consistently transforming nucleon-nucleon and three-nucleon potentials is relatively straightforward [16, 17]. Still, consistently SRG-transformed potentials have seen mixed success in nuclear structure calculations [56, 64–66], often facing substantial SRG resolution scale dependence and challenges in the simultaneous description of nuclei and nuclear matter.
- In parallel, a pragmatic approach that emerged was the SRG transformation of nucleon-nucleon potentials to low resolution followed by a refitting of the resolution-dependent short-range three-nucleon force couplings to ensure RG invariance of three- and four-body observables [30, 50]. Some Hamiltonians constructed this way have been very successful in calculations of nuclei up to ^{208}Pb (see Fig. 6).
- The success of low-resolution Hamiltonians constructed using RG methods has also motivated the use of low cutoffs in effective

field theories. Several established Hamiltonians employ low cutoffs of $\Lambda = 394\text{--}450$ MeV [45, 58, 66–68], which give them similar convergence properties to RG-transformed low-momentum Hamiltonians (see Fig. 6).

- Recently, in nuclear lattice effective field theory [69], wavefunction matching for nucleon-nucleon forces was developed [70] following established philosophies of RG transformations of nucleon-nucleon potentials. Problematic short-range interactions are transformed using a unitary transformation and matched to long-range interactions from effective field theory. The resulting Hamiltonians are amenable to the perturbative treatment used in lattice EFT calculations⁶ and have been able to provide a good description of bulk properties of nuclei up to ⁴⁰Ca.

6 Conclusion

The similarity renormalization group and low-resolution nuclear forces continue to play key roles in nuclear theory today [73]. Nuclear theory calculations are rapidly expanding their frontiers, computing superheavy isotopes, nuclei at the drip lines, fundamental interactions in nuclei, reactions in exotic systems, and properties of neutron-star matter. Improving our understanding of nuclear forces and developing more accurate low-resolution Hamiltonians will be essential to continued progress.

Data availability

Accompanying this chapter is a Python code `nn-srg` [20, 21] to allow readers to experiment with the SRG transformation of nucleon-nucleon potentials. Users can explore the momentum-space SRG transformation of nucleon-nucleon potentials, featuring both the AV18 and EM500 potentials, and test SRG scale invariance on deuteron binding energies and nucleon-nucleon phase shifts. `nn-srg` contains scripts to generate Figs. 1 and 2.

Acknowledgments

I am grateful to Scott Bogner, Dick Furnstahl, Kai Hebeler, Heiko Hergert, Robert Perry, Robert Roth, and Achim Schwenk for instruction, discussions, and research projects on the similarity renormalization group and to many more colleagues and collaborators for fruitful discussions on nuclear physics. I thank Francesca Bonaiti, Dick Furnstahl, Ulrich Heinz, and Thomas Papenbrock for valuable feedback on drafts of this chapter.

This work was supported by the U.S. Department of Energy, Office of Science, Office of Advanced Scientific Computing Research and Office of Nuclear Physics, Scientific Discovery through Advanced Computing (SciDAC) program (SciDAC-5 NUCLEI) and by the Laboratory Directed Research and Development Program of Oak Ridge National Laboratory, managed by UT-Battelle, LLC, for the U.S. Department of Energy. This research used resources of the Oak Ridge Leadership Computing Facility located at Oak Ridge National Laboratory, which is supported by the Office of Science of the Department of Energy under contract No. DE-AC05-00OR22725.

References

- [1] S. Weinberg, “Phenomenological Lagrangians,” *Phys. A: Stat. Mech. Appl.* **96**, 327 (1979).
- [2] E. Epelbaum, H.-W. Hammer, and U.-G. Meißner, “Modern theory of nuclear forces,” *Rev. Mod. Phys.* **81**, 1773 (2009).
- [3] R. Machleidt and D. R. Entem, “Chiral effective field theory and nuclear forces,” *Phys. Rep.* **503**, 1 (2011).
- [4] H.-W. Hammer, S. König, and U. van Kolck, “Nuclear effective field theory: Status and perspectives,” *Rev. Mod. Phys.* **92**, 025004 (2020).
- [5] K. G. Wilson and J. Kogut, “The renormalization group and the ϵ expansion,” *Phys. Rep.* **12**, 75 (1974).
- [6] S. K. Bogner, R. J. Furnstahl, and A. Schwenk, “From low-momentum interactions to nuclear structure,” *Prog. Part. Nucl. Phys.* **65**, 94 (2010).
- [7] S. D. Glazek and K. G. Wilson, “Perturbative renormalization group for Hamiltonians,” *Phys. Rev. D* **49**, 4214 (1994).
- [8] F. Wegner, “Flow-equations for Hamiltonians,” *Ann. Phys.* **506**, 77 (1994).
- [9] S. K. Bogner, R. J. Furnstahl, and R. J. Perry, “Similarity renormalization group for nucleon-nucleon interactions,” *Phys. Rev. C* **75**, 061001(R) (2007).
- [10] A. J. Tropiano, S. K. Bogner, and R. J. Furnstahl, “Short-range correlation physics at low renormalization group resolution,” *Phys. Rev. C* **104**, 034311 (2021).
- [11] E. Anderson, S. K. Bogner, R. J. Furnstahl, E. D. Jurgenson, R. J. Perry, and A. Schwenk, “Block diagonalization using SRG flow equations,” *Phys. Rev. C* **77**, 037001 (2008).
- [12] H. A. Bethe, “Theory of nuclear matter,” *Ann. Rev. Nucl. Part. Sci.* **21**, 93 (1971).
- [13] M. Lacombe, B. Loiseau, J. M. Richard, R. Vinh Mau, J. Côté, P. Pirès, and R. de Tourreil, “Parametrization of the Paris NN potential,” *Phys. Rev. C* **21**, 861 (1980).

⁶Nuclear lattice effective field theory treats many subleading interactions in perturbation theory. Recent work has extended fully nonperturbative coupled cluster and in-medium similarity renormalization group calculations to lattice bases [71, 72].

- [14] R. B. Wiringa, V. G. J. Stoks, and R. Schiavilla, "Accurate nucleon-nucleon potential with charge-independence breaking," *Phys. Rev. C* **51**, 38 (1995).
- [15] R. Machleidt, "High-precision, charge-dependent Bonn nucleon-nucleon potential," *Phys. Rev. C* **63**, 024001 (2001).
- [16] E. D. Jurgenson, P. Navrátil, and R. J. Furnstahl, "Evolution of nuclear many-body forces with the similarity renormalization group," *Phys. Rev. Lett.* **103**, 082501 (2009).
- [17] K. Hebeler, "Momentum-space evolution of chiral three-nucleon forces," *Phys. Rev. C* **85**, 021002(R) (2012).
- [18] S. D. Glazek and R. J. Perry, "The impact of bound states on similarity renormalization group transformations," *Phys. Rev. D* **78**, 045011 (2008).
- [19] K. A. Wendt, R. J. Furnstahl, and R. J. Perry, "Decoupling of spurious deep bound states with the similarity renormalization group," *Phys. Rev. C* **83**, 034005 (2011).
- [20] M. Heinz, "nn-srg," <https://github.com/cheshyre/nn-srg> (2025).
- [21] M. Heinz, "nn-srg: Similarity renormalization group evolution for nucleon-nucleon interactions (v1.0)," (2025).
- [22] D. R. Entem and R. Machleidt, "Accurate charge-dependent nucleon-nucleon potential at fourth order of chiral perturbation theory," *Phys. Rev. C* **68**, 041001(R) (2003).
- [23] S. K. Bogner, T. T. S. Kuo, A. Schwenk, D. R. Entem, and R. Machleidt, "Towards a model-independent low momentum nucleon-nucleon interaction," *Phys. Lett. B* **576**, 265 (2003).
- [24] S. K. Bogner, T. T. S. Kuo, and A. Schwenk, "Model-independent low momentum nucleon interaction from phase shift equivalence," *Phys. Rep.* **386**, 1 (2003).
- [25] B. Dainton, R. J. Furnstahl, and R. J. Perry, "Universality in Similarity Renormalization Group Evolved Potential Matrix Elements and T-Matrix Equivalence," *Phys. Rev. C* **89**, 014001 (2014).
- [26] H.-W. Hammer, A. Nogga, and A. Schwenk, "Colloquium: Three-body forces: From cold atoms to nuclei," *Rev. Mod. Phys.* **85**, 197 (2013).
- [27] K. Hebeler, J. D. Holt, J. Menéndez, and A. Schwenk, "Nuclear forces and their impact on neutron-rich nuclei and neutron-rich matter," *Annu. Rev. Nucl. Part. Sci.* **65**, 457 (2015).
- [28] K. Hebeler, "Three-nucleon forces: Implementation and applications to atomic nuclei and dense matter," *Phys. Rep.* **890**, 1 (2021).
- [29] R. Roth, J. Langhammer, A. Calci, S. Binder, and P. Navrátil, "Similarity-transformed chiral NN+3N interactions for the ab initio description of ^{12}C and ^{16}O ," *Phys. Rev. Lett.* **107**, 072501 (2011).
- [30] K. Hebeler, S. K. Bogner, R. J. Furnstahl, A. Nogga, and A. Schwenk, "Improved nuclear matter calculations from chiral low-momentum interactions," *Phys. Rev. C* **83**, 031301(R) (2011).
- [31] H. Hergert, "A guided tour of ab initio nuclear many-body theory," *Front. Phys.* **8**, 379 (2020).
- [32] G. Hagen, M. Hjorth-Jensen, G. R. Jansen, R. Machleidt, and T. Papenbrock, "Evolution of shell structure in neutron-rich calcium isotopes," *Phys. Rev. Lett.* **109**, 032502 (2012).
- [33] V. Somà, A. Cipollone, C. Barbieri, P. Navrátil, and T. Duguet, "Chiral two- and three-nucleon forces along medium-mass isotope chains," *Phys. Rev. C* **89**, 061301 (2014).
- [34] H. Hergert, S. Binder, A. Calci, J. Langhammer, and R. Roth, "Ab initio calculations of even oxygen isotopes with chiral two-plus-three-nucleon interactions," *Phys. Rev. Lett.* **110**, 242501 (2013).
- [35] G. Hagen, A. Ekström, C. Forssén, G. R. Jansen, W. Nazarewicz, T. Papenbrock, K. A. Wendt, S. Bacca, N. Barnea, B. Carlsson, C. Drischler, K. Hebeler, M. Hjorth-Jensen, M. Miorelli, G. Orlandini, A. Schwenk, and J. Simonis, "Neutron and weak-charge distributions of the ^{48}Ca nucleus," *Nat. Phys.* **12**, 186 (2016).
- [36] G. Hagen, G. R. Jansen, and T. Papenbrock, "Structure of ^{78}Ni from first-principles computations," *Phys. Rev. Lett.* **117**, 172501 (2016).
- [37] S. R. Stroberg, A. Calci, H. Hergert, J. D. Holt, S. K. Bogner, R. Roth, and A. Schwenk, "Nucleus-dependent valence-space approach to nuclear structure," *Phys. Rev. Lett.* **118**, 032502 (2017).
- [38] S. R. Stroberg, J. D. Holt, A. Schwenk, and J. Simonis, "Ab initio limits of atomic nuclei," *Phys. Rev. Lett.* **126**, 022501 (2021).
- [39] R. W. Fearick, P. von Neumann-Cosel, S. Bacca, J. Birkhan, F. Bonaiti, *et al.*, "Electric dipole polarizability of ^{40}Ca ," *Phys. Rev. Res.* **5**, L022044 (2023).
- [40] Z. H. Sun, A. Ekström, C. Forssén, G. Hagen, G. R. Jansen, and T. Papenbrock, "Multiscale physics of atomic nuclei from first principles," *Phys. Rev. X* **15**, 011028 (2025).
- [41] M. Heinz, T. Miyagi, S. R. Stroberg, A. Tichai, K. Hebeler, and A. Schwenk, "Improved structure of calcium isotopes from ab initio calculations," *Phys. Rev. C* **111**, 034311 (2025).
- [42] M. Heinz, M. Hoferichter, T. Miyagi, F. Nöel, and A. Schwenk, "Ab initio calculations of overlap integrals for $\mu \rightarrow e$ conversion in nuclei," *Phys. Lett. B* **871**, 139975 (2025).
- [43] T. Plies, M. Heinz, and A. Schwenk, "Uncertainties with low-resolution nuclear forces," (2025), [arXiv:2509.24671](https://arxiv.org/abs/2509.24671).
- [44] T. Miyagi, S. R. Stroberg, P. Navrátil, K. Hebeler, and J. D. Holt, "Converged ab initio calculations of heavy nuclei," *Phys. Rev. C* **105**, 014302 (2022).
- [45] B. S. Hu, W. G. Jiang, T. Miyagi, Z. H. Sun, A. Ekström, C. Forssén, G. Hagen, J. D. Holt, T. Papenbrock, S. R. Stroberg, and I. Vernon, "Ab initio predictions link the neutron skin of ^{208}Pb to nuclear forces," *Nat. Phys.* **18**, 1196 (2022).
- [46] K. Hebeler, V. Durant, J. Hoppe, M. Heinz, A. Schwenk, J. Simonis, and A. Tichai, "Normal ordering of three-nucleon interactions for ab initio calculations of heavy nuclei," *Phys. Rev. C* **107**, 024310 (2023).
- [47] M. Door, C.-H. Yeh, M. Heinz, F. Kirk, C. Lyu, *et al.*, "Probing new bosons and nuclear structure with ytterbium isotope shifts," *Phys. Rev. Lett.* **134**, 063002 (2025).
- [48] T. Miyagi, M. Heinz, and A. Schwenk, "Ab initio computations of the fourth-order charge density moments of ^{48}Ca and ^{208}Pb ," *Phys. Lett. B* **872**, 140032 (2026).
- [49] B. T. Reed, M. Heinz, P. Arthuis, A. Schwenk, and I. Tews, "Connecting relativistic density functional theory to microscopic calculations," *Phys. Rev. C* **112**, 034331 (2025).
- [50] P. Arthuis, K. Hebeler, and A. Schwenk, "Neutron-rich nuclei and neutron skins from chiral low-resolution interactions," (2024), [arXiv:2401.06675](https://arxiv.org/abs/2401.06675).
- [51] F. Bonaiti, G. Hagen, and T. Papenbrock, "Structure of the doubly magic nuclei ^{208}Pb and ^{266}Pb from ab initio computations," (2025), [arXiv:2508.14217](https://arxiv.org/abs/2508.14217).
- [52] G. Hagen, T. Papenbrock, M. Hjorth-Jensen, and D. J. Dean, "Coupled-cluster computations of atomic nuclei," *Rep. Prog. Phys.* **77**, 096302 (2014).
- [53] H. Hergert, S. K. Bogner, T. D. Morris, A. Schwenk, and K. Tsukiyama, "The in-medium similarity renormalization group: A novel ab initio method for nuclei," *Phys. Rep.* **621**, 165 (2016).
- [54] A. Tichai, R. Roth, and T. Duguet, "Many-body perturbation theories for finite nuclei," *Front. Phys.* **8**, 164 (2020).
- [55] V. Somà, "Self-consistent Green's function theory for atomic nuclei," *Front. Phys.* **8**, 340 (2020).

- [56] J. Hoppe, C. Drischler, K. Hebeler, A. Schwenk, and J. Simonis, "Probing chiral interactions up to next-to-next-to-next-to-leading order in medium-mass nuclei," *Phys. Rev. C* **100**, 024318 (2019).
- [57] K. Tsukiyama, S. K. Bogner, and A. Schwenk, "In-medium similarity renormalization group for nuclei," *Phys. Rev. Lett.* **106**, 222502 (2011).
- [58] W. G. Jiang, A. Ekström, C. Forssén, G. Hagen, G. R. Jansen, and T. Papenbrock, "Accurate bulk properties of nuclei from $A = 2$ to ∞ from potentials with Δ isobars," *Phys. Rev. C* **102**, 054301 (2020).
- [59] G. Hagen, D. J. Dean, M. Hjorth-Jensen, T. Papenbrock, and A. Schwenk, "Benchmark calculations for ${}^3\text{H}$, ${}^4\text{He}$, ${}^{16}\text{O}$, and ${}^{40}\text{Ca}$ with ab initio coupled-cluster theory," *Phys. Rev. C* **76**, 044305 (2007).
- [60] S. K. Bogner, R. J. Furnstahl, P. Maris, R. J. Perry, A. Schwenk, and J. P. Vary, "Convergence in the no-core shell model with low-momentum two-nucleon interactions," *Nucl. Phys. A* **801**, 21 (2008).
- [61] S. Quaglioni and P. Navrátil, "Ab initio many-body calculations of n - ${}^3\text{H}$, n - ${}^4\text{He}$, p - ${}^3,4\text{He}$, and n - ${}^{10}\text{Be}$ scattering," *Phys. Rev. Lett.* **101**, 092501 (2008).
- [62] H. Feldmeier, T. Neff, R. Roth, and J. Schnack, "A unitary correlation operator method," *Nucl. Phys. A* **632**, 61 (1998).
- [63] R. Roth, T. Neff, and H. Feldmeier, "Nuclear structure in the framework of the unitary correlation operator method," *Prog. Part. Nucl. Phys.* **65**, 50 (2010).
- [64] S. Binder, A. Calci, E. Epelbaum, R. J. Furnstahl, J. Golak, *et al.* (LENPIC Collaboration), "Few-nucleon and many-nucleon systems with semilocal coordinate-space regularized chiral nucleon-nucleon forces," *Phys. Rev. C* **98**, 014002 (2018).
- [65] T. Hüther, K. Vobig, K. Hebeler, R. Machleidt, and R. Roth, "Family of chiral two- plus three-nucleon interactions for accurate nuclear structure studies," *Phys. Lett. B* **808**, 135651 (2020).
- [66] V. Somà, P. Navrátil, F. Raimondi, C. Barbieri, and T. Duguet, "Novel chiral Hamiltonian and observables in light and medium-mass nuclei," *Phys. Rev. C* **101**, 014318 (2020).
- [67] R. Roth, S. Binder, K. Vobig, A. Calci, J. Langhammer, and P. Navrátil, "Medium-mass nuclei with normal-ordered chiral NN+3N interactions," *Phys. Rev. Lett.* **109**, 052501 (2012).
- [68] A. Ekström, G. R. Jansen, K. A. Wendt, G. Hagen, T. Papenbrock, B. D. Carlsson, C. Forssén, M. Hjorth-Jensen, P. Navrátil, and W. Nazarewicz, "Accurate nuclear radii and binding energies from a chiral interaction," *Phys. Rev. C* **91**, 051301(R) (2015).
- [69] D. Lee, "Lattice simulations for few- and many-body systems," *Prog. Part. Nucl. Phys.* **63**, 117 (2009).
- [70] S. Elhatisari, L. Bovermann, Y.-Z. Ma, E. Epelbaum, D. Frame, *et al.*, "Wavefunction matching for solving quantum many-body problems," *Nature* **630**, 59 (2024).
- [71] M. Rothman, B. Johnson-Toth, F. Bonaiti, G. Hagen, M. Heinz, and T. Papenbrock, "Exactness of the normal-ordered two-body truncation of three-nucleon forces," *Phys. Rev. C* **112**, L051301 (2025).
- [72] M. Rothman, B. Johnson-Toth, G. Hagen, M. Heinz, and T. Papenbrock, "NuLattice: Ab initio computations of atomic nuclei on lattices," *Eur. Phys. J. A* **62**, 28 (2026), [arXiv:2509.08771](https://arxiv.org/abs/2509.08771).
- [73] I. Tews, Z. Davoudi, A. Ekström, J. D. Holt, K. Becker, *et al.*, "Nuclear forces for precision nuclear physics: A collection of perspectives," *Few-Body Sys.* **63**, 67 (2022).